PROCEEDINGS, Twenty-First Workshop on Geothermal Reservoir Engineering
Stanford University, Stanford, California, January 22-24, 1996
SGP-TR-151

NUMERICAL INVESTIGATION OF PRESSURE TRANSIENT RESPONSES OF A WELL PENETRATING A DEEP GEOTHERMAL RESERVOIR AT SUPER-CRITICAL CONDITIONS

Yusaku Yano and Tsuneo Ishido

Geological Survey of Japan
1-1-3 Higashi, Tsukuba
305 Japan

ABSTRACT

Numerical simulations were carried out to predict pressure transients in a hypothetical deep geothermal well which penetrates a reservoir at super-critical conditions. Production at about 4000 m depth was assumed. In many cases, two-phase conditions develop due to high temperature and production-induced pressure decrease. Several cases in which single-phase conditions are maintained were studied in detail. Pressure transients are influenced by the reservoir temperature distribution - in particular, a temperature distribution with subcritical conditions at the well but supercritical conditions farther away causes a characteristic nonlinear pressure response which is influenced by the large compressibility and small kinematic viscosity near the critical point.

INTRODUCTION

Deep geothermal reservoirs (4,000 meters depth and more) are important targets for future development of geothermal resources in Japan. NEDO (the New Energy and Industrial Technology Development Organization) is now drilling a 4,000 m well in the Kakkonda geothermal area. Production tests will be undertaken if a permeable fracture system is encountered at depth. GSJ (the Geological Survey of Japan) is carrying out a research program which is closely linked to NEDO's project, in which an evaluation of the deep reservoir will be performed. To this end, we have begun a fundamental study of the production-test response likely to be observed in the deep reservoir. Although actual production tests have not yet begun, we can investigate fluid properties and pressure transients in the deep reservoir at very high temperature and pressure using a simple reservoir model. Numerical simulation techniques are necessary for this investigation because fluid properties exhibit highly non-linear changes in this temperature-pressure range.

FLUID PROPERTIES IN DEEP RESERVOIRS

In the Kakkonda field, NEDO's deep test well has already reached very high temperature (449 ℃ or more) at a depth of 3,729 m (Uchida, et al., 1995). However, no permeability was encountered at that depth, and side tracking is now being planned. Therefore, no production tests have yet been performed, and there are presently no measurements of deep fluid properties.

Hypothetical deep reservoir models are used hereafter for our analysis, in anticipation of real field data to be acquired in the near future. Assuming a conductive temperature profile for a 4,000 m well in which the bottom hole temperature is 500 ℃, the stable hydrostatic bottomhole pressure should be roughly 27.5 MPa assuming that the water table is at the ground surface. Thus, bottomhole conditions are above the critical point for pure water.

For our numerical simulation study, we used the STAR general-purpose geothermal reservoir simulator (Pritchett, 1995), incorporating the HOTH2O equation of state package (Pritchett, 1994) for simulation of high pressure and temperature conditions. HOTH2O treats pure water for pressures to one kilobar (100 MPa) and temperatures to 800 ℃. The critical point

is defined as 374.15 ℃ and 22.12 MPa in the HOTH2O package. Figure 1 shows how temperaturedepends on pressure and specific internal energy; the shaded area is the two-phase region within which water and steam can coexist. Above the critical point (shown as "C" in Figure 1), there is no distinction between the liquid and vapor phases. Near the critical point, the physical properties of water tend to change drastically with small changes in temperature and/or pressure, and some properties become singular at the critical point. Theoretically, as the critical point is approached, the constant pressure specific heat, coefficient of volume expansion, compressibility, and thermal conductivity become infinite (e.g. Dunn and Hardee, 1981; Hayba and Ingebritsen, 1994).

Laboratory experiments by Dunn and Hardee (1981) found a substantial enhancement of heat transfer rates near the critical point. Cox and Pruess (1990) tried to simulate this experimental result using the MULKOM reservoir simulator, but were unable to quantitatively reproduce the full extent of the enhancement of heat transfer rate. We made some preliminary tests using

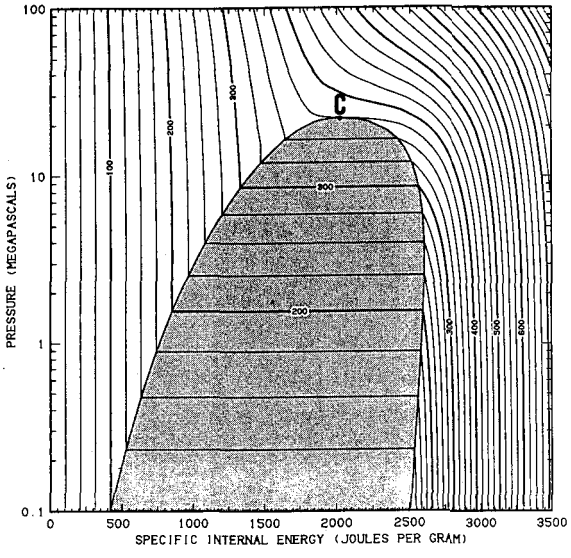

Fig. 1. Dependence of temperature on pressure and specific internal energy based on HOTH2O package data. Temperatures in degrees Celsus. Shaded area indicates two-phase region.

STAR, and obtained results similar to those of Cox and Pruess using similar simulation parameters. The discrepancy between experiments and calculations appears to arise from various effects which were not incorporated in either simulation.

NUMERICAL SIMULATION OF PRODUCTION TESTS FROM DEEP RESERVOIRS

A simple hypothetical deep geothermal reservoir model was used for our numerical study, as illustrated in Figure 2; pertinent parameter values are listed in Table 1. We consider a horizontal single-layer homogeneous porous-medium reservoir containing a single fully-penetrating production well which may be regarded as a line-sink. The outer radius is sufficient that the system may be considered infinite in lateral extent. Both upper and lower boundaries are impermeable and insulated.

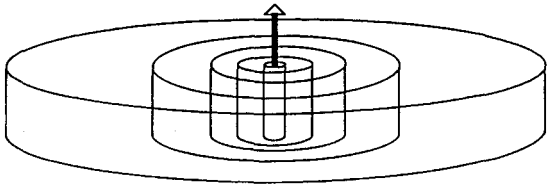

Fig. 2. Numerical simulation model.

Table 1. Model parameters used for the numerical simulation of production tests from a deep reservoir.

****

Reservoir geometry

Horizontal layer : Thickness = 100 m

Numerical blocks : r(1)=0.1m,

$\Delta r(i+1) = 1.3 \times \Delta r(i)$

r(max) = r(40) = 12,039m

Well block: $k = 10^{-10}$ m^2, ϕ =0.99

Reservoir blocks: $k = 10^{-14}$ m^2, ϕ =0.05

Common rock parameters:

rock grain density = 2.7 g/cm^3

rock grain heat capacity = 1000 joules/kg℃

rock grain thermal conductivity = 2.5 W/m℃

****

The initial temperature distribution, the initial pressure, and the production well discharge rate were the free parameters selected for the study; pressure changes with time in the well block are of primary interest. A large variety of cases characterized by different parameter values was considered. Most of the early cases used parameter values which resulted in the development of two-phase zones around the well during production. These results are difficult to interpret. In this paper, we concentrate on the cases which remained single-phase throughout.

In Figure 3, three cases (A, B and C) of pressure drawdown are shown. For these three cases, the same production rate (15.7 kg/sec), production interval duration (10^6 sec; 278 hours), and initial pressure (30 MPa) were used, and only the initial temperature distribution was varied. In all cases, a skin zone of high permeability (1 Darcy) is used (blocks 2-5; to 0.9 meters), to avoid generation of a two-phase zone.

Case A used a homogeneous initial temperature distribution of 300 ℃. In Case B, the initial temperature is heterogeneous, and equal to 300 ℃ for radii out to 82 meters (out to block 21) and 400 ℃ beyond that distance. In Case C, the initial temperature

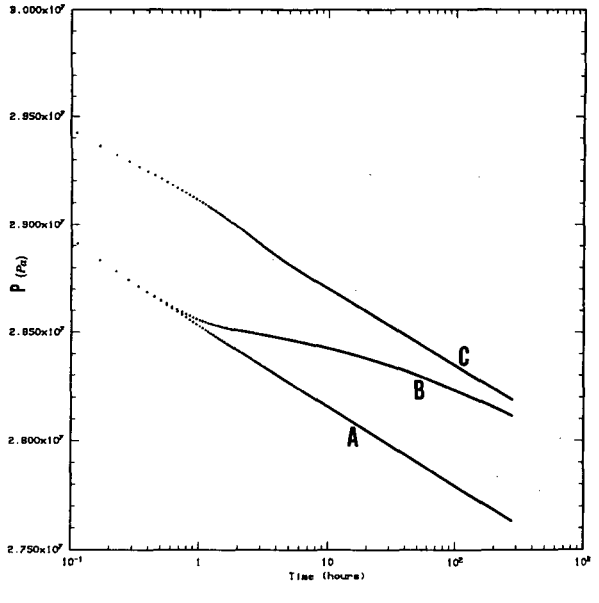

Fig. 3. Simulated pressure drawdowns with different initial temperature distributions.

is equal to 400 ℃ everywhere. Comparing the three drawdown histories in Figure 3, it is evident that Cases A and C have similar slopes, although their absolute pressures are different. Also, the earlier part of the Case B drawdown is the same as that of Case A, whereas at late times Case B approaches Case C.

The pressure drawdown (ΔP) for a radial flow reservoir is given by:

$$\Delta P = m\,[\log t + \log(4k/\phi\,\mu\,cr^2) - 0.251 + 2s\log e] \quad (1)$$

where m is the slope on the semi-log plot, t is time since production began, k, ϕ, μ, and c are permeability, porosity, dynamic viscosity of fluid, and total compressibility respectively, and r is radial distance from the well and s is skin factor. The slope m is

$$m = 2.303\,W\nu/4\pi kh \quad (2)$$

where W is mass flow rate, ν is the kinematic viscosity, and h is the reservoir thickness. All three cases in Figure 3 have the same W and kh. At 30 MPa, the kinematic viscosity of water at 300 ℃ is 1.24×10^{-7} m^2/sec, and that at 400 ℃ is 1.23×10^{-7} m^2/sec. Therefore, a similar slope (m) is obtained for Cases A and C. The difference of the absolute values of pressure for both cases arises from the difference in water compressibility at 30 MPa pressure. The compressibility of water at 400 ℃ (Case C) is much greater than at 300 ℃ (Case A), which results in less pressure decrease for Case C.

The reservoir temperature distribution does not change significantly during the production test in Case B. At early times in this case fluid is being withdrawn from storage at small radii (300 ℃), whereas at later times fluid is withdrawn from the hotter (400 ℃) outer zone. This causes the shift in the curve for Case B shown in Figure 3.

In Figure 4, Horner plots of build-up pressure transients for the three cases are shown. Build-up was simulated for 2×10^6 sec (556 hours) of shut-in time.

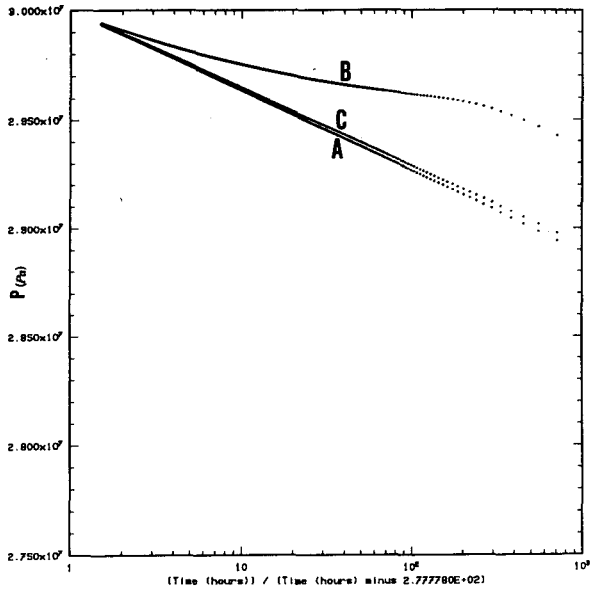

Fig. 4. Horner plots of the simulated buildup pressure transients.

Horner-times of 100 and 10 correspond to 2.8 hours and 30.9 hours of shut-in time, respectively. The buildup pressures of Cases A and C become almost identical in the later stage of the build up. The buildup pressure is expressed as

$$\Delta P = m \log((t + \Delta t) / \Delta t) \qquad (3)$$

where $(t + \Delta t) / \Delta t$ is Horner time. Buildup response is independent of compressibility, so that kinematic viscosity (which influences the slope m - see Eq. 2) is the only parameter which differentiates the transient buildup response between Cases A and C at late times (small Horner times).

Equation (3) cannot be used for Case B, since fluid properties (particularly compressibility) are heterogeneous in that case. In Case B, the later stage of drawdown is dominated by the influence of the 400 ℃ region, the early stage of buildup is dominated by the influence of the 300 ℃ region, and again the later stage of buildup is influenced by the 400 ℃ region. Therefore, even though there is little difference between viscosities at 300 ℃ and 400 ℃, the difference of compressibilities makes the behavior of Case B significantly different from that of Cases A and C as shown in Figure 4.

Figure 5 shows pressure drawdown behavior for seven cases which differ only in the initial (homogeneous) reservoir temperature assumed; other parameters are the same as Cases A and C. Starting from 200 ℃, pressure decrease becomes smaller with increasing reservoir temperature up to about 400 ℃; for higher temperatures, however, pressure decrease increases markedly with increasing temperature. Between 400 ℃ and 500 ℃, the kinematic viscosity of water increases from 1.23×10^{-7} m²/sec to 2.75×10^{-7} m²/sec, while there is little change in kinematic viscosity between 300 ℃ and 400 ℃; a minimum (1.16×10^{-7} m²/sec) is reached near 375 ℃. The kinematic viscosity at 200 ℃ is 1.59×10^{-7} m²/sec.

Figure 6 shows pressure drawdown transients for four different cases, all with initial reservoir temperature of 450 ℃, but with different initial reservoir pressures. As the initial reservoir pressure increases from 25 MPa to 35 MPa, the kinematic viscosity of water decreases

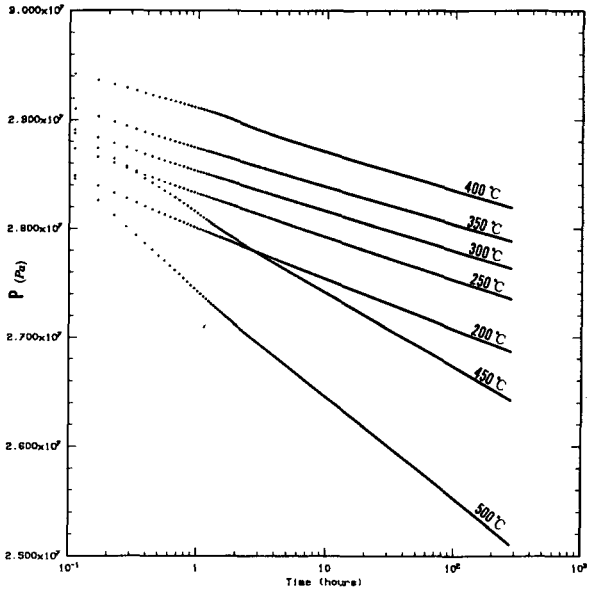

Fig. 5. Simulated pressure drawdowns with different reservoir temperatures. Initial reservoir pressure is 30MPa.

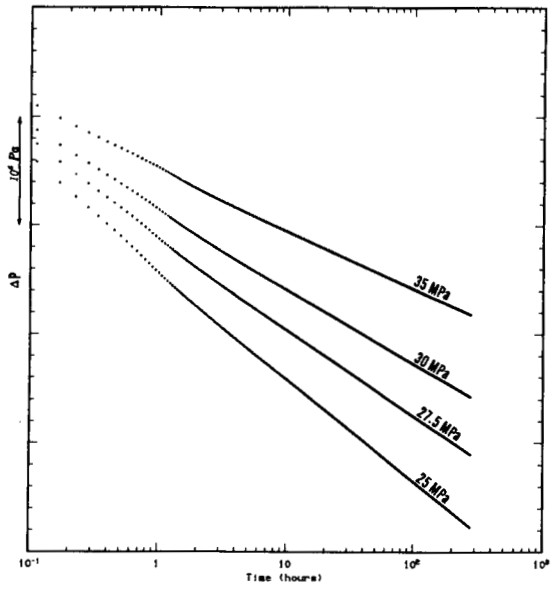

Fig. 6. Simulated pressure drawdowns with different initial reservoir pressure. Initial reservoir temperature is 450 ℃.

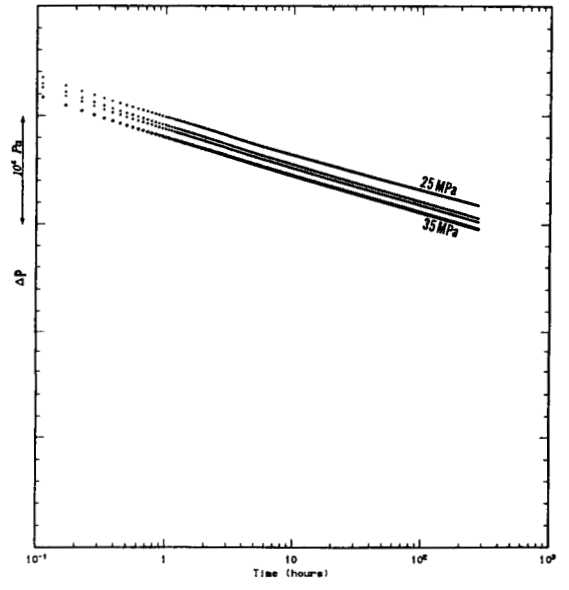

Fig. 7. Simulated pressure drawdowns with different initial reservoir pressure. Initial reservoir temperature is 375℃.

from 2.65 × 10^{-7} m^2/sec to 1.68 × 10^{-7} m^2/sec, at 450 ℃. Figure 7 shows pressure drawdown transients of four similar cases, except that the initial reservoir temperature is lower (375 ℃). In this case, the kinematic viscosity lies between 1.15 and 1.16 × $10^{-7}m^2$/sec for all cases, so the pressure differences are very small; slopes are nearly identical, and the pressure amplitude differs only because of compressibility differences.

SUMMARY

If the temperature distribution in a geothermal reservoir is heterogeneous, drawdown and buildup pressures can exhibit highly nonlinear behavior as shown in Figures 3 and 4. In this case, there is no vapor phase present in the reservoir, but the existence of a super-critical zone brings about the complicated pressure behavior. Pressure responses are mainly affected by non-linear changes of compressibility and fluid kinematic viscosity. These results suggest that it may be possible to identify super-critical reservoir conditions based on non-linear pressure transient response.

The pressure response of a deep reservoir is very sensitive to temperature, as shown in Figure 5, especially above the critical point. The sensitivity of pressure response to initial reservoir pressure depends on the initial reservoir temperature, as shown in Figures 6 and 7. If the temperature is far above the critical point, the pressure response is very sensitive to the initial pressure. Therefore, we need precise information about the temperature and pressure of the deep reservoir for the analysis of pressure transient data.

ACKNOWLEDGEMENTS

The authors deeply appreciate John W. Pritchett for his many useful comments.

REFERENCES

Cox, B. L. and Pruess, K. (1990) Numerical experiments on convective heat transfer in water-saturated porous media at near-critical conditions. Transport in Porous Media 5, 299-323.

Dunn, J. C. and Hardee, H. C. (1981) Superconvecting geothermal zones. Journal of Volcanology and Geothermal Research, 11, 189-201.

Hayba, D. O. and Ingebritsen S. E. (1994) Flow near the critical point : Examination of some pressure-enthalpy paths. Proc. 19th Workshop Geothermal Reservoir Engineering, Stanford University. 83-89.

Pritchett, J. W. (1994) "HOTH2O" A description of H_2O properties to one kilobar and 800 ℃ for use with the STAR geothermal reservoir simulator. SSS-TR-94-14730, S-Cubed, La Jolla.

Pritchett, J. W. (1995) STAR: A geothermal reservoir simulation system. Proc. World Geothermal Congress 1995, 4, 2959-2960.

Uchida, T., Muraoka, H., Yagi, M., Sasaki, M., Kamenosono, H., Miyazaki, S., Doi, N., Sasada, M., and Sawaki, T. (1995) An update of "Deep-Seated Resources" survey. 1995 Abstracts with Programs Annual Meeting of the Geothermal Research Society of Japan, P18.